catalysts

MDPI

Article

Preparation of $Fe_3O_4/TiO_2/C$ Nanocomposites and Their Application in Fenton-Like Catalysis for Dye Decoloration

Xiaoyang Liu, Qian Zhang, Baowei Yu, Ruihan Wu, Jinxia Mai, Ruijue Wang, Lingyun Chen and Sheng-Tao Yang *

College of Chemistry and Environment Protection Engineering, Southwest University for Nationalities, Chengdu 610041, China; 13908064583@163.com (X.L.); qianzhang1018@sina.com (Q.Z.); yubaowei816@sina.com (B.Y.); 13688435898@163.com (R.W.); m18328594292@163.com (J.M.); sheor_wang@sina.com (R.W.); 13558844990@163.com (L.C.)

* Correspondence: yangst@pku.edu.cn; Tel.: +86-28-8552-2269

Academic Editor: Keith Hohn

Received: 21 July 2016; Accepted: 12 September 2016; Published: 20 September 2016

Abstract: Fe^{2+}-H_2O_2 Fenton system is widely applied in water treatment nowadays, but the acidification and sludge generation are crucial problems to be solved. Herein, we report that $Fe_3O_4/TiO_2/C$ nanocomposites (FTCNCs) were able to catalyze the decomposition of H_2O_2 at neutral pH and can be applied in dye decoloration. FTCNCs were prepared by precipitating TiO_2 on Fe_3O_4 cores via the hydrolysis of tetrabutyl titanate followed by the hydrothermal dehydrogenization of glucose to deposit carbon on Fe_3O_4/TiO_2. The decoloration of methylene blue (MB) in the FTCNC-H_2O_2 Fenton-like system was monitored to reflect the catalytic activity of FTCNC. The radical generation capability was analyzed by electron spin resonance. Our results indicated that FTCNC-H_2O_2 Fenton-like system was efficient in decolorizing MB, and the radicals led to the near complete oxidation of MB. The FTCNC-H_2O_2 Fenton-like system could be used in a wide pH range of 4–9. A greater catalyst amount, a higher H_2O_2 concentration, and a higher temperature accelerated the decoloration kinetics. FTCNCs showed good activity after the regeneration of 8 cycles. The implication to the practical applications of FTCNCs in water treatment is discussed.

Keywords: $Fe_3O_4/TiO_2/C$ nanocomposites; Fenton-like catalyst; heterogeneous catalysis; advanced oxidation processes; water treatment

1. Introduction

Advanced oxidation processes (AOPs) are important technologies for water treatment, in particular for the pollutants that are hardly biotransformed in active sludge treatment. Generally, oxidative radicals or other intermediates are generated during AOP treatment and the oxidative species oxidize the electron-enriched organic pollutants [1–3]. Among the most commonly applied AOPs, the Fe^{2+}-H_2O_2 Fenton system has attracted great interest and has been used for water remediation on a large scale. Despite the success in practical applications, the Fe^{2+}-H_2O_2 Fenton system has several marked disadvantages that require further improvements. The most vital one is that the optimal pH of the Fe^{2+}-H_2O_2 Fenton system is acidic (at pH 3). Thus, polluted water has to be acidified before treatment and followed by neutralization after treatment. Another drawback is that the Fe^{2+}-H_2O_2 Fenton system requires a stoichiometric amount of iron. The iron ions are hard to remove and generate a high degree of sludge [4,5]. The iron containing sludge should be further treated to avoid environmental hazards.

In recent years, heterogeneous Fenton-like catalysis has been developed as a new alternative to the traditional Fe^{2+}-H_2O_2 Fenton system. Typically, heterogeneous Fenton-like catalysts are microsized or nanosized and contain Fe or other metal elements, where the surface metal atoms catalyze the decomposition of H_2O_2. Many heterogeneous catalysts have been reported to catalyze the decomposition of H_2O_2 for water treatment [6–12]. Both iron-containing and iron-free catalysts have been studied, and external energy supply (e.g., sonication [13,14], electricity [2] and light irradiation [9,15–17]) is adopted in many cases to enhance the performance of heterogeneous catalysis. For instance, humic acid modified Fe_3O_4 served as a Fenton-like catalyst and catalyzed the degradation of sulfathiazole [6]. Fe_3O_4/CeO_2 nanocomposites catalyzed the degradation of methyl orange under microwave irradiation [8]. The MnO_4 microstructure could be used for the degradation of methylene blue (MB) [18]. To simplify the conditions, much research has been dedicated to developing nanoparticles as Fenton-like catalysts without an external energy supply. However, such attempts usually worked under acidic pH levels (around pH 3).

Previously, we reported the doping of TiO_2 on a Fe_3O_4 nanoparticle surface to shift the applicable pH to near-neutral [19]. However, the stability and regeneration of TiO_2-doped Fe_3O_4 nanoparticles were poor. Here, we prepared $Fe_3O_4/TiO_2/C$ nanocomposites (FTCNC) as a Fenton-like catalyst for the decomposition of H_2O_2 and tested the performance of the FTCNC-H_2O_2 system in the decoloration of MB. FTCNCs were carefully characterized before used, and the catalytic performance was compared with naked Fe_3O_4 at a neutral pH level. The influences of radical scavengers, catalyst amount, H_2O_2 concentration, pH, and temperature were investigated. The regeneration capability was analyzed up to 8 cycles. The implication on the applications of FTCNCs in water treatment is discussed.

2. Results and Discussion

2.1. Characterization of FTCNCs

FTCNCs were characterized by multiple techniques before use. The morphology of FTCNCs was investigated under transmission electron microscopy (TEM, Figure 1). It was recognized that the particles were irregular. The size distribution of particles was very wide with large particles of about 20 nm in diameter and small ones of about 5 nm. The particles aggregated to form larger composites due to the magnetic attraction and the high surface energy, even though the aggregate was loosely packed and the pores were presented under TEM, which would allow the diffusion of small molecules onto the inner surface of FTCNC. The surface area was measured by the Brunauer–Emmett–Teller (BET) technique, and the value was 96.5 m^2/g. The large surface area was consistent with the small particle sizes. The N_2 adsorption/desorption isotherm curve of FTCNCs followed type IV (Figure 2a), indicating the adsorption hysteresis nature. The magnetic property measurement showed the ferromagnetic character of FTCNC, which should be due to the nanoscale sizes. The saturated magnetization of FTCNCs was 48.5 emu/g, similar to other modified Fe_3O_4 nanoparticles. The ferromagnetic character was good for the applications of FTCNC, because FTCNCs could disperse better without an external magnet during the catalysis and could be magnetically separated after the reaction with the external magnet.

The chemical composition was analyzed by X-ray photoelectron spectroscopy (XPS). O (43.5 atom %), C (38.6 atom %), Fe (14.0 atom %), and Ti (3.9 atom %) were detected in FTCNC. The low Ti content indicated that the TiO_2 only partially covered the surface of Fe_3O_4, consistent with the TEM observation, where no core-shell structure was presented. The contents of both Fe and Ti reduced after the hydrothermal reaction, suggesting that Fe and Ti were partially lost during the reaction to form some nonmagnetic substances. The XPS spectra of C, Fe, and Ti are shown in Figure 3. According to the analyses, the carbon atoms could be divided into C–C (56%), C–O (34%), and C=O (10%). The C1s spectrum suggested that the glucose was carbonized, but many oxygen atoms were retained. The existence of Ti^{4+} was confirmed by the typical Ti $2p_{3/2}$ and Ti $2p_{1/2}$ peaks. The Fe^{3+}/Fe^{2+} ratio was calculated from the peak areas of Fe $2p_{3/2}$ as 1.35:1, smaller than those of Fe_3O_4 (2:1) and

the starting Fe^{3+}/Fe^{2+} ratio (1.5:1), likely due to the chemical reduction during the hydrothermal reaction. The groups containing oxygen, distinguished from the C1s XPS spectrum, was confirmed by the infrared (IR) spectrum. The peak at 3390 cm^{-1} is attributed to –OH and –COOH groups. The tiny peak at 2970 cm^{-1} was due to the remnant C–H bonds on the residues of glucose. The graphite carbon (C=C) is reflected by the peak at 1620 cm^{-1}. The peaks at 579 cm^{-1} and 432 cm^{-1} were assigned to Ti–O and Fe–O.

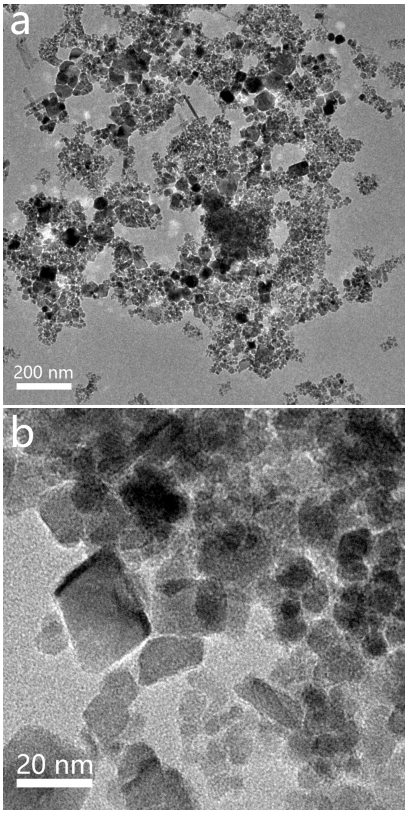

Figure 1. TEM images of $Fe_3O_4/TiO_2/C$ nanocomposites (FTCNCs). (**a**) Low magnification; (**b**) higher magnification.

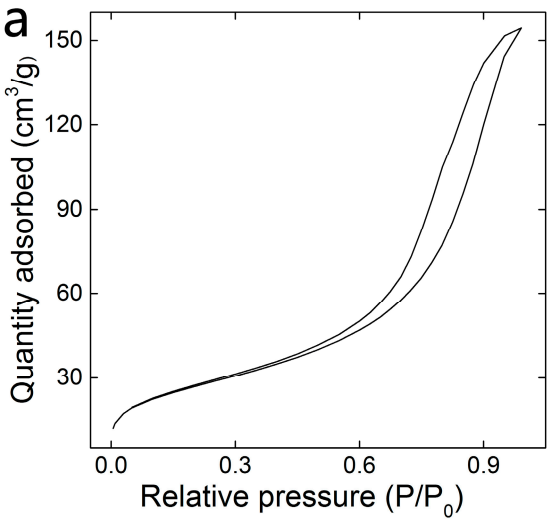

Figure 2. *Cont.*

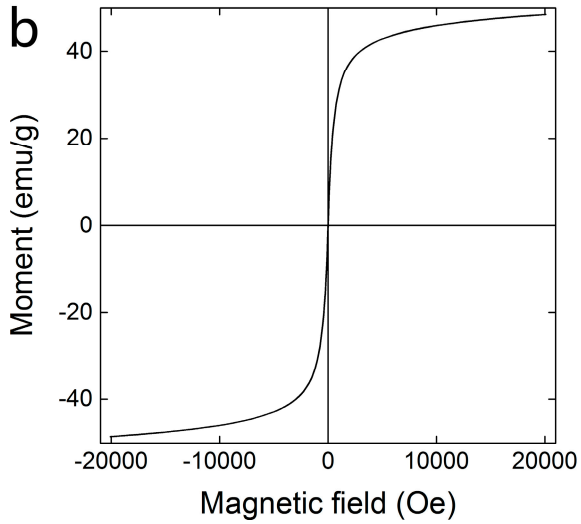

Figure 2. Nitrogen adsorption isotherm (**a**) and magnetic hysteresis loop (**b**) of FTCNCs.

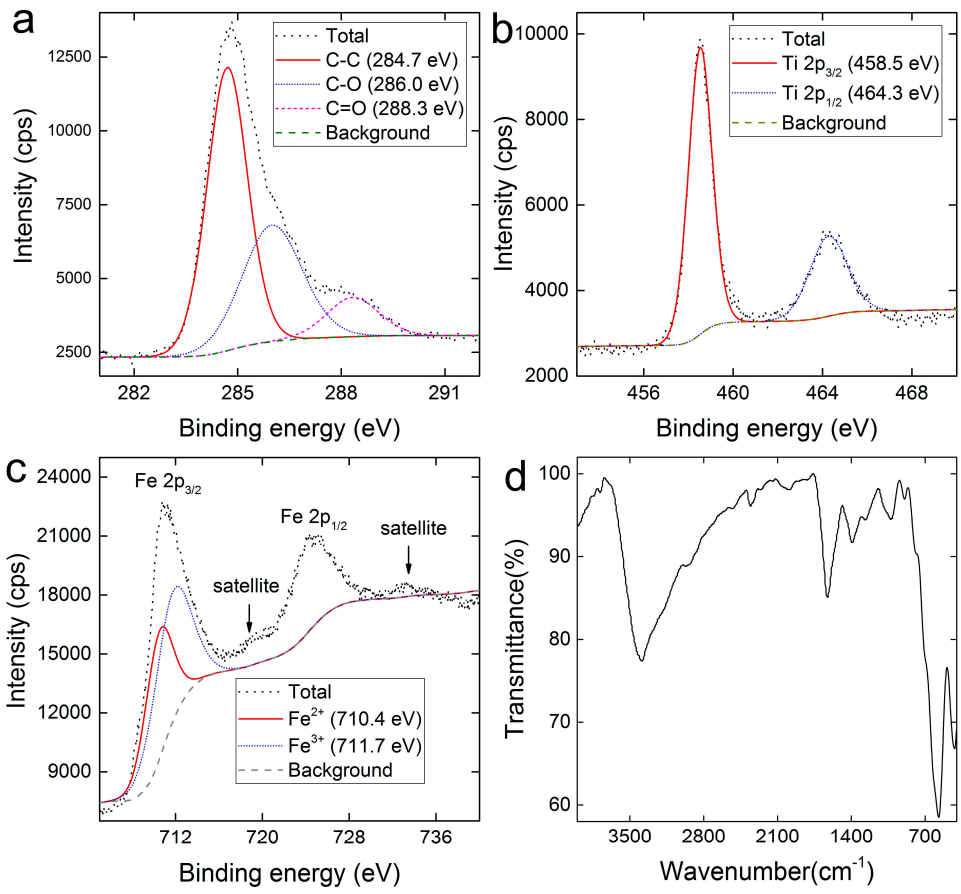

Figure 3. XPS and IR spectra of FTCNCs. (**a**) C1s XPS spectrum; (**b**) Ti2p XPS spectrum; (**c**) Fe2p XPS spectrum; (**d**) IR spectrum.

2.2. Decoloration of MB in the FTCNC-H_2O_2 Fenton-Like System

The FTCNC-H_2O_2 Fenton-like system showed good capability in decolorizing MB (Figure 4a), suggesting the high catalytic activity of FTCNCs in the decomposition of H_2O_2. The decoloration

was carried out at near-neutral pH (pH 6) [19]. In contrast, very limited decoloration was observed in the Fe_3O_4-H_2O_2 system and the catalyst-free system. The decoloration efficiency of MB was 82% for the FTCNC-H_2O_2 Fenton-like system, 9.4% for the Fe_3O_4-H_2O_2 system and 6.7% for the catalyst-free system. The results clearly indicate that the co-incorporation of TiO_2 and C shifted the working pH of Fe_3O_4 to near-neutral. We also analyzed the kinetics of decoloration. The corresponding kinetics constant k values were calculated as 0.011 min^{-1} for the FTCNC-H_2O_2 Fenton-like system, 0.00055 min^{-1} for the Fe_3O_4-H_2O_2 system, and 0.00031 min^{-1} for the catalyst-free system. The k value for the FTCNC-H_2O_2 Fenton-like system was two magnitudes higher than the other two. The kinetics of the FTCNC-H_2O_2-MB system was competitive with other systems using various nanocatalysts. For example, the Fe_3O_4@SiO_2-H_2O_2-MB system had a k value of 0.020 min^{-1} [7]. The k values of the FePt-H_2O_2-MB system were in the range of 0.0033–0.023 min^{-1} at the pH value of 5.5 [20]. The Ti-doped Fe_3O_4-H_2O_2-MB system had a similar k value (0.0165 min^{-1}). From the perspective of kinetics, the incorporation of carbon did not improve the performance of TiO_2-doped Fe_3O_4 [19]. The major improvements induced by carbon incorporation were the sample stability and regeneration. The TiO_2-doped Fe_3O_4 was vulnerable during storage, while FTCNCs could be stored under room temperature for more than two months. The regeneration of FTCNCs was much better than the TiO_2-doped Fe_3O_4. Moreover, we also measured the chemical oxygen demand (COD) to verify the complete oxidation of MB (Figure 4c). The trends of the optical density and COD decreases were nearly identical, which suggested that the decoloration of MB was mainly due to the complete oxidation of MB into CO_2 [20–25].

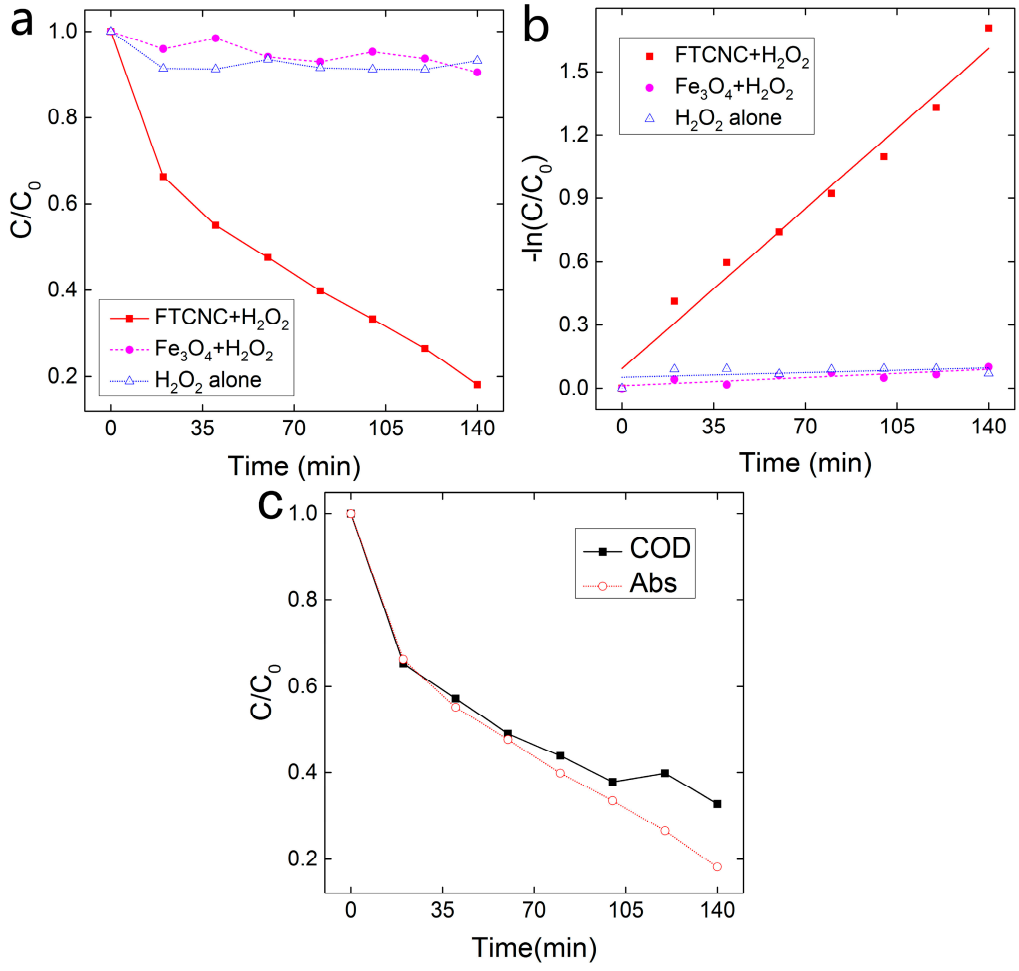

Figure 4. Catalytic activity of FTCNCs. (**a**) Decoloration efficiency; (**b**) kinetics analyses; (**c**) COD (chemical oxygen demanding) removal.

Generally, many Fenton systems generate oxidative radicals and other non-radical species [26]. To confirm the existence of ·OH radicals in the FTCNC-H_2O_2 Fenton-like system, the electron spin resonance (ESR) spectra of the FTCNC-H_2O_2 Fenton-like system were recorded [21]. As shown in Figure 5, the 4-fold characteristic peaks of 5,5-dimethyl-1-pyrroline-*N*-oxide (DMPO)-·OH adduct was observed with the intensity ratio of 1:2:2:1 in the ESR spectra of the FTCNC-H_2O_2 Fenton-like system. More radicals were generated at 10 min than those at 5 min, which was reflected by the higher intensity. The radicals could be partially quenched by tertiary butanol, a typical scavenger for radicals (Figure 5b). Along with the increase of tertiary butanol concentration, the catalytic activity of FTCNCs was inhibited. However, it should be noted that, even at very high tertiary butanol (0.909 mol/L, 3878 times of that of MB), the decoloration was still meaningful with a k value of 0.0066 min^{-1}. The resistance of the FTCNC-H_2O_2 system to tertiary butanol should be due to the incorporation of TiO_2 and C. It was speculated that radicals were generated on the surface of the FTCNCs, and the radicals then diffused from the surface to the solution phase, forming higher radical concentrations around the surface of the FTCNCs. MB interacted more intensively with the FTCNCs than tertiary butanol; thus, more MB was concentrated around the surface of the FTCNCs and reached the radicals prior to tertiary butanol [21]. Therefore, radicals oxidized MB before they diffused into the solution phase, where the extinction of radicals by tertiary butanol occurred. The tolerance of the FTCNC-H_2O_2 system to radical scavengers was important for practical applications, because there might be radical scavengers in polluted water, and no pre-purification is required. Beyond the radical process, according to the literature, there might also be non-radical processes involved. Recently, van Eldik et al. found a new mechanistic aspect of Fenton reactions in which not only hydroxyl radicals but also $Fe^{III}(^{-}O_2H)_{aq}$ were involved [26]. Thus, H_2O_2 decomposed to generate several oxidative species that further oxidized the MB molecules.

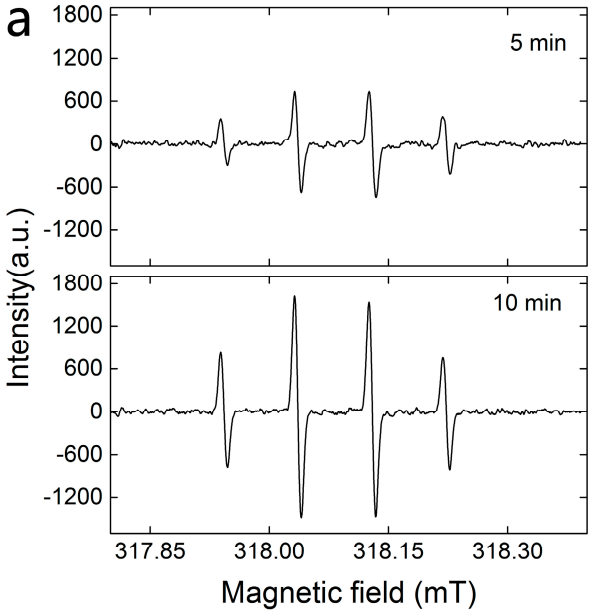

Figure 5. *Cont.*

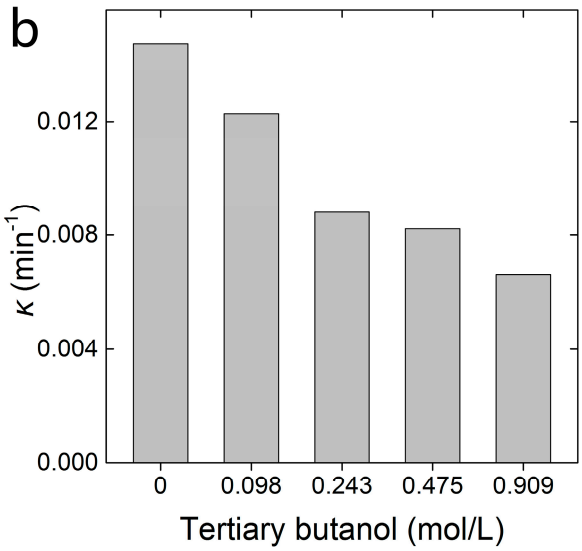

Figure 5. Resistance of the FTCNC-H_2O_2 Fenton-like system against radical scavenger tertiary butanol. (**a**) ESR spectra of FTCNC-H_2O_2 Fenton-like system at 5 and 10 min; (**b**) influence of tertiary butanol.

Beyond the good resistance to radical scavengers, the FTCNC-H_2O_2 Fenton-like system was capable of working at different pH levels and temperatures. We investigated the influence of four factors, namely catalyst amount, H_2O_2 volume, pH, and temperature. As described in Figure 6, more FTCNCs and H_2O_2 accelerated the decoloration. This was reasonable from the kinetics perspective and widely observed in heterogeneous Fenton reactions [8]. At a high catalyst amount, the increase of decoloration kinetics slowed down, which suggested that the diffusion of MB toward the active sites of FTCNCs controlled the reaction kinetics. The optimal pH for the FTCNC-H_2O_2 Fenton-like system was pH 6. The FTCNC-H_2O_2 Fenton-like system also worked in the pH range of 4–9. A slightly acidic environment (pH 4–6) seemed much better than neutral and basic environments (pH 7–9). The wide applicable pH range implied that the FTCNC-H_2O_2 Fenton-like system can be used at various pH values without pH adjustment. This obviously overcame the main drawback of the Fe^{2+}-H_2O_2 system, which only worked at pH 3. The shift of optimal pH toward neutral should be attributed to the doping of TiO_2 on Fe_3O_4. Previously, we have demonstrated that TiO_2 doping could push the applicable pH of the Fenton reaction to near-neutral [19], while C coating did not change the optimal pH level. According to the experiences of chelators and SiO_2 [21], possible mechanism could be that –OH groups of TiO_2 chelated with Fe^{2+} and the chelation shifted the optimal pH level. It is well known that the point of zero charge (PZC) of TiO_2 was near pH 6 [27]. At a pH level higher than 6, the hydroxyl groups on TiO_2 deprotonated to form $–O^-$, making the surface negative. By reducing the pH to 6, hydroxyl groups were protonated to form –OH and the surface charge was neutral. Further reduction of pH generated $–OH_2^+$, making the surface positive. At a low pH level, the positive charge of $–OH_2^+$ repelled MB toward the surface due to electrostatic repulsion. At a high pH level, the lack of proton inhibited the Fenton-like reaction. At the optimal pH, close to the PZC of TiO_2, the status of surface hydroxyl groups was –OH, which can chelate with Fe^{2+}. By increasing the temperature, the decoloration was significantly accelerated. The increase in temperature accelerated the diffusion of MB toward active sites and more molecules reached the activation energy [28]. By fitting the kinetics constant and temperature to the Arrhenius equation (R = 0.995), the activation energy of decoloration was 26.35 kJ/mol. The small activation energy was consistent with the fast decoloration.

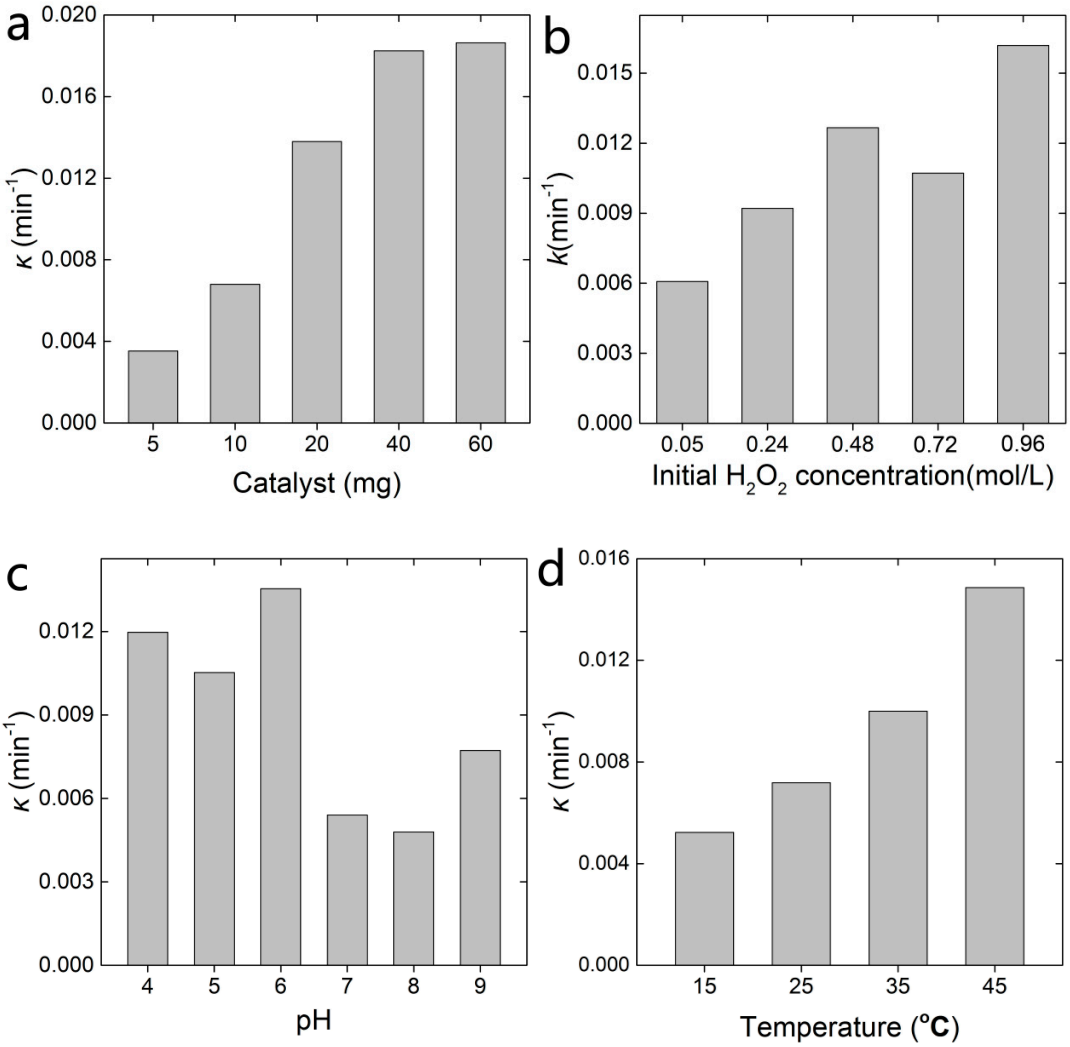

Figure 6. Influencing factors on the decoloration performance of the FTCNC-H_2O_2 Fenton-like system. (**a**) Catalyst amount; (**b**) H_2O_2 volume; (**c**) pH; (**d**) temperature.

2.3. The Recycle of FTCNCs

The regeneration of catalyst after decoloration is essential in reducing the operating cost and environmental burden. As shown in Figure 7, the regeneration led to a slight decrease in decoloration efficiency of the FTCNC-H_2O_2 Fenton-like system. After the first round of recycle, the decoloration efficiency kept nearly constant, indicating that some vulnerable active sites of FTCNCs were lost in the first round. The remnant sites were much more stable and survived in the following seven rounds of recycle. Compared with the TiO_2-doped Fe_3O_4 [19], FTCNCs showed much better regeneration capability. The improvement of regeneration should be attributed to the incorporation of carbon. Previously, the sacrificial role of graphene oxide (GO) was confirmed in the regeneration of GO–Fe_3O_4 [29]. The carbon atoms of GO were oxidized during the Fenton reaction; therefore, Fe^{2+} remained non-oxidized. A similar phenomenon has been observed in $Fe_3O_4/SiO_2/C$ nanocomposites, where carbon incorporation enhanced the regeneration of Fe_3O_4/SiO_2 [20]. Overall, upon the incorporation of carbon, FTCNCs had good regeneration ability and is thus more promising for practical applications [21,28].

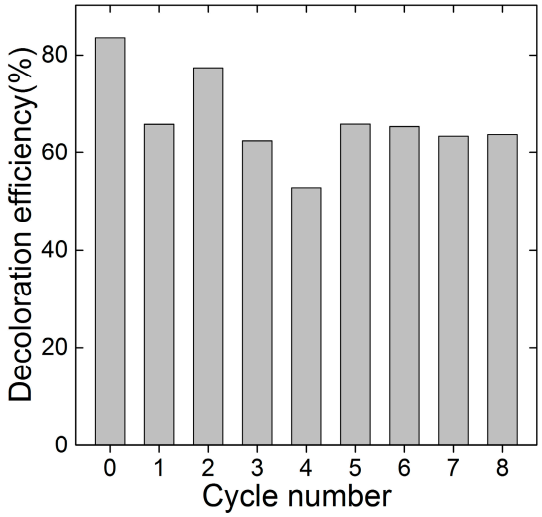

Figure 7. Recycle of FTCNCs after the decoloration of MB (methylene blue).

3. Materials and Methods

3.1. Preparation of FTCNCs

$FeCl_2 \cdot 4H_2O$ (0.45 g) and $FeCl_3 \cdot 6H_2O$ (0.90 g) were dissolved in 40 mL of deionized water. The pH was adjusted to pH 12 with a NaOH solution under vigorous stirring. After aging for 1 h, the magnetic components were collected and washed with deionized water. The as-prepared Fe_3O_4 was dried for TiO_2 doping. A portion of 0.1 g Fe_3O_4 was sonicated in a mixture of 20 mL of alcohol and 100 μL of $NH_3 \cdot H_2O$ for 5 min. A mixture of 1.62 mL of tetrabutyl titanate and 20 mL of alcohol was added dropwise into the Fe_3O_4 suspension. The suspension was then shaken at 100 rpm at 35 °C for 6 h. The TiO_2-doped Fe_3O_4 was magnetically separated, washed, and dried. Then, 0.4 g of TiO_2-doped Fe_3O_4, 1.6 g of glucose, and 60 mL of deionized water were placed in a Teflon tube (Hengli Co., Chengdu, China) and heated to 160 °C for 6 h. The precipitates were magnetically separated to collect FTCNCs. FTCNCs were washed and lyophilized before characterization and catalysis. FTCNCs were characterized by TEM (Tecnai G2 20, FEI, Hillsboro, OR, USA), the BET technique (ASAP2010, Micromeritics, Norcross, GA, USA), a magnetometer (MPMS XL-7 tesla, Quantum Design, San Diego, CA, USA), XPS (Kratos, Stretford, UK), and an IR spectrometer (Magna-IR 750, Nicolet, Rhinelander, WI, USA).

3.2. Decoloration of MB in FTCNC-H_2O_2 Fenton-Like System

20 mg of FTCNCs were added to a 20-mL MB solution (75 mg/L, pH 6) and shaken at 110 rpm at 35 °C for 2 h to reach the adsorption equilibrium. The absorbance of the MB solution was recorded at 664 nm on a UV-vis spectrometer (UV-1800, Mapada, Shanghai, China) as A_0. Then, 1 mL of H_2O_2 was added to the system (the final concentration of H_2O_2 was 0.48 mol/L) and was kept shaking. At each interval of 20 min, the absorbance was recorded as A_t. The decoloration efficiency was calculated with Equation (1). The decoloration kinetics were analyzed with Equation (2). The corresponding COD values of water samples were measured using a Hach reagent (low range 3–150 mg/L) on the Hach DR900 (Hach Co., Loveland, CO, USA). For comparison, the decoloration of MB in the Fe_3O_4-H_2O_2 system and the catalyst-free system was determined following the same protocol.

$$Decoloration\ efficiency = (1 - \frac{A_t}{A_0}) \times 100\% \quad (1)$$

$$-\ln(C/C_0) = kt \quad (2)$$

3.3. Resistance to Radical Scavengers

The generation of ·OH radicals was monitored on aJES FA200 (JEOL, Tokyo, Japan) facility with a microwave bridge (receiver gain: 1×10^5; modulation amplitude: 2 gauss; microwave power: 4 mW; modulation frequency: 100 kHz) (JEOL, Tokyo, Japan). Briefly, 100 mL of sample solution was collected from the reaction system (the FTCNC-H_2O_2 system without MB) at 5 min and 10 min. An amount of 20 mL of 0.2 mol/L DMPO was added to the solution to form a DMPO-·OH adduct.

To test the resistance of the FTCNC-H_2O_2 system to radical scavengers, 20 mg of FTCNCs, 1 mL of H_2O_2 (final concentration of 0.48 mol/L), and 20 mL of MB solution (75 mg/L, pH 6) were added with different volumes of tertiary butanol. The decoloration was monitored as described above.

3.4. Influencing Factors

The influencing factors including catalyst amount, H_2O_2 volume, pH, and temperature were investigated. For the catalyst amount, the FTCNC-H_2O_2 system was set as 5–60 mg of FTCNCs, 20 mL of MB solution (75 mg/L, pH 6), and 1 mL of H_2O_2 (final concentration of 0.48 mol/L). The decoloration was carried out at 35 °C. For the H_2O_2 volume, the FTCNC-H_2O_2 system was set as 20 mg of FTCNCs, 20 mL of MB solution (75 mg/L, pH 6), and 0.1–2 mL of H_2O_2 (final concentrations of 0.05–0.96 mol/L). The decoloration was also carried out at 35 °C. For pH, the FTCNC-H_2O_2 system was set as 20 mg of FTCNCs, 20 mL of MB solution (75 mg/L, pH 4–9), and 1 mL of H_2O_2 (final concentration of 0.48 mol/L). The decoloration was performed at 35 °C. For temperature, the FTCNC-H_2O_2 system was set as 20 mg of FTCNCs, 20 mL of MB solution (75 mg/L, pH 6), and 1 mL of H_2O_2 (final concentration of 0.48 mol/L). The decoloration was carried out at 15–45 °C. The decoloration kinetic constants were obtained with Equation (2) for comparison.

3.5. Regeneration of FTCNC

The used FTCNCs were washed with alcohol and water three times, and the effluent was nearly colorless. After magnetic separation, regenerated FTCNCs were lyophilized for a catalytic activity assay. The regeneration was repeated for 8 cycles.

4. Conclusions

In summary, FTCNCs of high catalytic activity were successfully prepared for the decomposition of H_2O_2, where the FTCNC-H_2O_2 Fenton-like system was used successfully for the decoloration of dyes in water treatment. The FTCNC-H_2O_2 Fenton-like system showed a much higher performance than the naked Fe_3O_4-H_2O_2 system, indicating that surface modification was crucial in improving the catalytic activity under neutral pH values. The good tolerance against radical scavengers and pH changes suggested that the FTCNC-H_2O_2 Fenton-like system might be stable in treating variations of polluted water. The regeneration of FTCNCs would markedly reduce the operating cost of the FTCNC-H_2O_2 Fenton-like system. We hope that our findings benefit the development of environmental nanotechnology and water treatment.

Acknowledgments: This work was supported by the Top-notch Young Talents Program of China, the China Natural Science Foundation (No. 201307101), and the Innovation Scientific Research Program for Graduates in Southwest University for Nationalities (No. CX2016SZ053).

Author Contributions: S.-T. Yang conceived and designed the experiments; X. Liu, Q. Zhang, and J. Mai performed the experiments; X. Liu, R. Wang, and S.-T. Yang analyzed the data; B. Yu and R. Wu contributed analysis tools; all authors wrote the paper.

Conflicts of Interest: The authors declare no conflict of interest.

References

1. Sires, I.; Brillas, E. Remediation of water pollution caused by pharmaceutical residues based on electrochemical separation and degradation technologies: A review. *Environ. Int.* **2012**, *40*, 212–229. [CrossRef] [PubMed]
2. Feng, L.; van Hullebusch, E.D.; Rodrigo, M.A.; Esposito, G.; Oturan, M.A. Removal of residual anti-inflammatory and analgesic pharmaceuticals from aqueous systems by electrochemical advanced oxidation processes: A review. *Chem. Eng. J.* **2013**, *228*, 944–964. [CrossRef]
3. Naumczyk, J.; Bogacki, J.; Marcinowski, P.; Kowalik, P. Cosmetic waste water treatment by coagulation and advanced oxidation processes. *Environ. Technol.* **2013**, *35*, 541–548. [CrossRef] [PubMed]
4. Neyens, E.; Baeyens, J. A review of classic Fenton's peroxidation as an advanced oxidation technique. *J. Hazard. Mater.* **2003**, *98*, 33–50. [CrossRef]
5. Xu, H.Y.; Prasad, M.; He, X.L.; Shan, L.W.; Qi, S.Y. Discoloration of Rhodamine B dyeing waste water by schorl-catalyzed Fenton-like reaction. *Sci. Chin. Technol. Sci.* **2009**, *52*, 3054–3060. [CrossRef]
6. Niu, H.Y.; Zhang, D.; Zhang, S.X.; Zhang, X.L.; Meng, Z.F.; Cai, Y.Q. Humic acid coated Fe_3O_4 magnetic nanoparticles as highly efficient Fenton-like catalyst for complete mineralization of sulfathiazole. *J. Hazard. Mater.* **2011**, *190*, 559–565. [CrossRef] [PubMed]
7. Yang, S.T.; Zhang, W.; Xie, J.R.; Liao, R.; Zhang, X.L.; Yu, B.W.; Wu, R.H.; Liu, X.Y.; Li, H.L.; Guo, Z. Fe_3O_4@SiO_2 nanoparticles as high-performance Fenton-like catalyst in neutral environment. *RSC Adv.* **2015**, *5*, 5458–5463. [CrossRef]
8. Bai, D.; Yan, P. Magnetic nanoscaled Fe_3O_4 as an efficient and reusable heterogeneous catalyst for degradation of methyl orange in microwave-enhanced Fenton-like system. *Appl. Mech. Mater.* **2014**, *448–453*, 830–833.
9. Xu, L.J.; Wang, J.L. Magnetic nanoscaled Fe_3O_4/CeO_2 composite as an efficient Fenton-Like heterogeneous catalyst for degradation of 4-chlorophenol. *Environ. Sci. Technol.* **2012**, *46*, 10145–10153. [CrossRef] [PubMed]
10. Hammouda, S.B.; Adhoum, N.; Monser, L. Synthesis of magnetic alginate beads based on Fe_3O_4 nanoparticles for the removal of 3-methylindole from aqueous solution using Fenton process. *J. Hazard. Mater.* **2015**, *294*, 128–136. [CrossRef] [PubMed]
11. Zhang, T.; Yu, S.R.; Feng, H.X. Fenton-like mineralization of anion surfactant by Fe_2O_3/attapulgite catalyst. *Adv. Mater. Res.* **2012**, *399–401*, 1392–1395. [CrossRef]
12. Luo, M.S.; Yuan, S.H.; Tong, M.; Liao, P.; Xie, W.J.; Xu, X.F. An integrated catalyst of Pd supported on magnetic Fe_3O_4 nanoparticles: Simultaneous production of H_2O_2 and Fe^{2+} for efficient electro-Fenton degradation of organic contaminants. *Water Res.* **2014**, *48*, 190–199. [CrossRef] [PubMed]
13. Huang, R.X.; Fang, Z.Q.; Fang, X.B.; Tsang, E.P. Ultrasonic Fenton-like catalytic degradation of bisphenol A by ferroferric oxide (Fe_3O_4) nanoparticles prepared from steel pickling waste liquor. *J. Colloid Interface Sci.* **2014**, *436*, 258–266. [CrossRef] [PubMed]
14. Wang, C.K.; Shih, Y. Degradation and detoxification of diazinon by sono-Fenton and sono-Fenton-like processes. *Sep. Purif. Technol.* **2015**, *140*, 6–12. [CrossRef]
15. Paola, A.D.; Bellardita, M.; Palmisano, L. Brookite, the least known TiO_2 photocatalyst. *Catalysts* **2013**, *3*, 36–73. [CrossRef]
16. Yasuda, M.; Tomo, T.; Hirata, S.; Shiragami, T.; Matsumoto, T. Neighboring hetero-atom assistance of sacrificial amines to hydrogen evolution using Pt-loaded TiO_2-photocatalyst. *Catalysts* **2014**, *4*, 162–173. [CrossRef]
17. Gil, S.; Garcia-Vargas, J.M.; Liotta, L.F.; Pantaleo, G.; Ousmane, M.; Retailleau, L.; Giroir-Fendler, A. Catalytic oxidation of propene over Pd catalysts supported on CeO_2, TiO_2, Al_2O_3 and M/Al_2O_3 oxides (*M* = Ce, Ti, Fe, Mn). *Catalysts* **2015**, *5*, 671–689. [CrossRef]
18. Wang, Y.; Zhu, L.; Yang, X.; Shao, E.; Deng, X.; Liu, N.; Wu, M. Facile synthesis of three-dimensional Mn_3O_4 hierarchical microstructures and their application in the degradation of methylene blue. *J. Mater. Chem. A* **2015**, *3*, 2934–2941. [CrossRef]
19. Yang, S.T.; Yang, L.J.; Liu, X.Y.; Xie, J.R.; Zhang, X.L.; Yu, B.W.; Wu, R.H.; Li, H.L.; Chen, L.Y.; Liu, J.H. TiO_2-doped Fe_3O_4 nanoparticles as high-performance Fenton-like catalyst for dye decoloration. *Sci. Chin. Technol. Sci.* **2015**, *58*, 858–863. [CrossRef]
20. Hsieh, S.; Lin, P.Y. FePt nanoparticles as heterogeneous Fenton-like catalysts for hydrogen peroxide decomposition and the decolorization of methylene blue. *J. Nanopart. Res.* **2012**, *14*, 956–965. [CrossRef]

21. Wang, R.J.; Liu, X.Y.; Wu, R.H.; Yu, B.W.; Li, H.L.; Zhang, X.L.; Xie, J.R.; Yang, S.T. $Fe_3O_4/SiO_2/C$ nanocomposite as a high-performance Fenton-like catalyst in a neutral environment. *RSC Adv.* **2016**, *6*, 8594–8600. [CrossRef]
22. Zhou, Q.; Gong, W.Q.; Yang, D.J.; Xie, C.X.; Li, Y.B.; Liu, X.F.; Bai, C.P.; Wang, R. Assessment of the biosorption characteristics of a spent cottonseed husk substrate for the decolorization of methylene blue. *Clean Soil Air Water* **2011**, *39*, 1087–1094. [CrossRef]
23. Low, L.W.; Teng, T.T.; Alkarkhi, A.F.; Ahmad, A.; Morad, N. Optimization of the adsorption conditions for the decolorization and COD reduction of methylene blue aqueous solution using low-cost adsorbent. *Water Air Soil Pollut.* **2011**, *214*, 185–195. [CrossRef]
24. Min, Y.L.; Zhang, K.; Zhao, W.; Zheng, F.C.; Chen, Y.C.; Zhang, Y.G. Enhanced chemical interaction between TiO_2 and graphene oxide for photocatalytic decolorization of methylene blue. *Chem. Eng. J.* **2012**, *193–194*, 203–210. [CrossRef]
25. Zhang, C.F.; Qiu, L.G.; Ke, F.; Zhu, Y.J.; Yuan, Y.P.; Xu, G.S.; Jiang, X. A novel magnetic recyclable photocatalyst based on metal-organic framework Fe_3O_4@MIL-100(Fe) core-shell for the decolorization of methylene blue dye. *J. Mater. Chem. A* **2013**, *1*, 14329–14334. [CrossRef]
26. Rachmilovich-Calis, S.; Masarwa, A.; Meyerstein, N.; Meyerstein, D.; van Eldik, R. New mechanistic aspects of the Fenton reaction. *Chem. Eur. J.* **2009**, *15*, 8303–8309. [CrossRef] [PubMed]
27. Bertus, L.M.; Carcel, R.A. Prediction of TiO_2 and WO_3 nanopowders surface charge by the evaluation of point of zero charge (PZC). *Environ. Eng. Manag. J.* **2011**, *10*, 1021–1026.
28. Zhang, X.L.; He, M.L.; Liu, J.H.; Liao, R.; Zhao, L.Q.; Xie, J.R.; Wang, R.J.; Yang, S.T.; Wang, H.F.; Liu, Y.F. Fe_3O_4@C nanoparticles as high-performance Fenton-like catalyst for dye decoloration. *Chin. Sci. Bull.* **2014**, *59*, 3406–3412. [CrossRef]
29. Zubir, N.A.; Yacou, C.; Motuzas, J.; Zhang, X.; Zhao, X.; da Costa, J.C.D. The sacrificial role of graphene oxide in stabilising a Fenton-like catalyst GO-Fe_3O_4. *Chem. Commun.* **2015**, *51*, 9291–9293. [CrossRef] [PubMed]